Angewandte Chemie
Eine Zeitschrift der Gesellschaft Deutscher Chemiker

Supporting Information



69451 Weinheim, Germany

# Label-Free Quantitative Imaging of Cholesterol in Intact Tissues by Hyperspectral Stimulated Raman Scattering Microscopy**

*Ping Wang, Junjie Li, Pu Wang, Chun-Rui Hu, Delong Zhang, Michael Sturek,* and Ji-Xin Cheng**

anie_201306234_sm_miscellaneous_information.pdf

## Experimental setup

Our hyperspectral SRS microscope (Figure S1a) employed a dual output femtosecond pulse laser (InSight DeepSee, Spectra-Physics, Mountain View, CA) with a repetition rate at 80 MHz. The 120-fs tunable laser was tuned to 883 nm, served as the pump beam $\omega_p$. The other 220-fs laser with fixed power of 500 mW and wavelength of 1040 nm was used as the Stokes beam $\omega_s$. For heterodyne detection, the Stokes beam intensity was modulated by an acousto-optical modulator (AOM, 1205-C, Isomet, Springfield, VA) at 2.25 MHz. The pulse shaping technology[1] was employed for intra-pulse spectral manipulation. One 4f pulse shaper was installed in the Stokes beam to narrow down the spectral width of the 220-fs laser. After the optical modulator and the pulse shaper, full width at half maximum (FWHM) of the pulse was measured to be 2.3 ps by an autocorrelator and the laser power was measured to be 50 mW. Another 4f pulse shaper was installed in the pump beam for intra-pulse wavelength scanning with a motorized translation stage (T-LS28E, Zaber, Vancouver, Canada) at the Fourier plane of the pulse shaper. By controlling the slit width, a spectral FWHM width of ~0.2 nm was obtained for the pump beam (Figure S1b). The maximum pump beam power was 50 mW, measured at 883 nm. The pump and Stokes beams were collinearly combined and directed into a homebuilt laser scanning upright microscope. A water immersion objective lens (UPlanSApo, Olympus, Tokyo, Japan) with numerical aperture of 1.2 focused the lasers into the sample. The photons were collected by an oil condenser (NA=1.4). The pump beam was selected by two bandpass filters (HQ825/150m, Chroma, Bellows Falls, VT), and was detected by a photodiode (S3994-01, Hamamatsu, Japan) equipped with a resonant circuit[2] that selectively amplifies the signal at the optical modulation frequency. The stimulated Raman loss signal was then extracted by a digital lock-in amplifier (HF2LI, Zurich Instrument, Zurich, Switzerland).[3] The DC output voltage from the resonant circuit, which represents the laser power, and the X channel voltage from the lock-in amplifier, which represents the SRS signal, were sampled by a DAQ card (PCI 6251, National Instruments, Austin, TX). A Labview platform synchronized scanning of wavelength with stacking of XY-Ω (Ω: Raman shift) images. Hyperspectral SRS imaging was performed by varying Raman shift from 1620 to 1800 $cm^{-1}$, which covers the acyl and sterol C=C stretch bands in lipid, the amide I band in protein, and the C=O band in ester. The estimated the spectral resolution of our system is 12 $cm^{-1}$. Each SRS image contained 200 x 200 pixels. The pixel dwell time was 10 μs for phantoms, 20 μs for emulsions, and 40 μs per pixel for arteries.

## Specimen preparation

Pure cholesterol crystal (Sigma Grade, ≥ 99%), glyceryl trioleate (Sigma Grade, ≥ 99%) and BSA were purchased from Sigma-Aldrich (St. Louis, MO). A droplet of glyceryl trioleate oil, cholesterol crystal and BSA powder were mixed and sealed between two glass coverslips right before SRS imaging.

Lipid droplet emulsions were prepared by solvent evaporation method. Briefly, cholesteryl oleate (Sigma) and glyceryl trioleate were both dissolved in acetone at the same concentration (10 mM). The cholesteryl oleate and glyceryl trioleate solutions were mixed together at various volume ratios. The mixtures were added to deionized water at a volume ratio of 1:20, supplemented with 0.05% Tween-20 surfactant. Lipid droplets formed during magnetic stirring for 10 min. A drop of emulsion was sandwiched between two glass coverslips and sealed right before imaging.

Atherosclerotic arteries were harvested from metabolic syndrome Ossabaw pigs. Briefly, the pigs were fed hypercaloric, atherogenic diet composed of 2% cholesterol, 20% kcal from fructose, and 43% kcal from hydrogenated soybean oil, coconut oil, and lard.[4] Carotid arteries with atherosclerotic plaque were harvested and preserved in 10% phosphate-buffered formalin after being cut to 50 μm thick sections. The artery slices were washed with phosphate-buffered saline and then sandwiched between two glass coverslips before SRS imaging.

## MCR algorithm

MCR[5] is a bilinear model capable of decomposing a measured spectral data set **D** into concentration profiles and spectra of chemical components, represented by matrices **C** and $\mathbf{S}^\mathbf{T}$,

$$\mathbf{D} = \mathbf{C}\,\mathbf{S}^\mathbf{T} + \mathbf{E}. \qquad (1)$$

Here, T means the transpose of matrix of **S**. **E** is the residual matrix or experimental error. The input to MCR is the dataset **D** and the reference spectra of each component. **S** contains the output spectra of all fitted components. The output concentration of a chemical component at each pixel is expressed as percentage relative to the intensity of the MCR optimized spectrum. Giving initial estimate of pure spectra either from principal component analysis or prior knowledge, an alternating least squares algorithm calculates **C** and **S** by Eq. (1) iteratively until the results optimally fit the data matrix **D**. Non negativity on both concentration and spectra profiles is applied as a constraint during the alternating least squares iteration.

Data augmentation was applied for cholesteryl ester quantification to reduce ambiguity associated with MCR decomposition.[5d] The augmentation matrix composed of repeating SRS spectra of acyl C=C, sterol C=C and ester group C=O bands was added to spectral dataset **D**. The enhanced weight on pure reference spectra ensured MCR algorithm to selectively recover concentration profiles for corresponding Raman bands from experimental dataset **D**. The flow chart of MCR can be found in supplementary Figure S2.

## Supporting references (more than 10 authors)


[2] P. Duewell, H. Kono, K. J. Rayner, C. M. Sirois, G. Vladimer, F. G. Bauernfeind, G. S. Abela, L. Franchi, G. Nunez, M. Schnurr, T. Espevik, E. Lien, K. A. Fitzgerald, K. L. Rock, K. J. Moore, S. D. Wright, V. Hornung, E. Latz, *Nature* **2010**, *464*, 1357-1361.

[11k] M. Paar, C. Jüngst, N. A. Steiner, C. Magnes, F. Sinner, D. Kolb, A. Lass, R. Zimmermann, A. Zumbusch, S. D. Kohlwein, H. Wolinski, *J. Biol. Chem.* **2012**, *287*, 11164-11173.

## *Supplementary Figures*

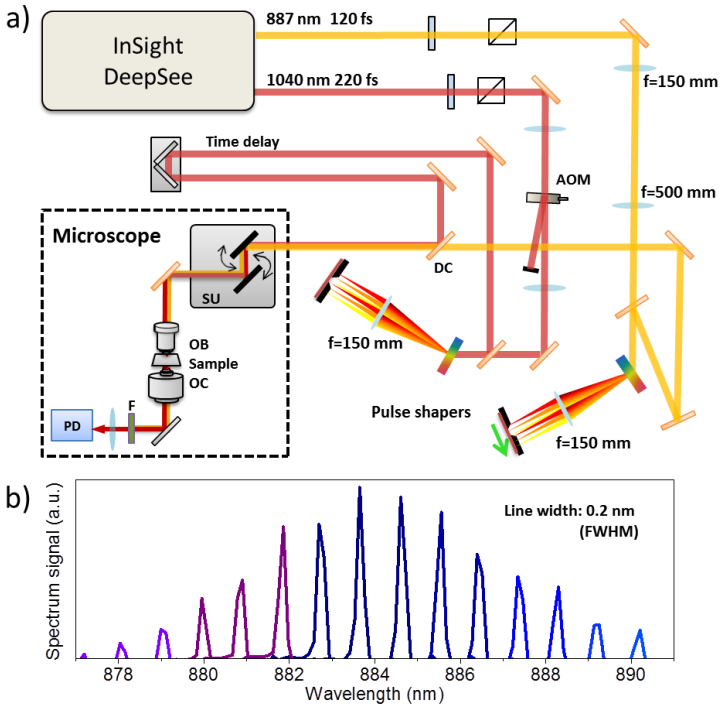


***Figure S1.*** Experimental setup. a) Schematic of hyperspectral stimulated Raman scattering microscope. DC: Dichroic combiner; SU: Scanning unit; OB: Objective; OC: Oil condenser; F: Bandpass filter; PD: Photodiode. b) Spectra of pump beam measured after the intra-pulse scanning pulse shaper.

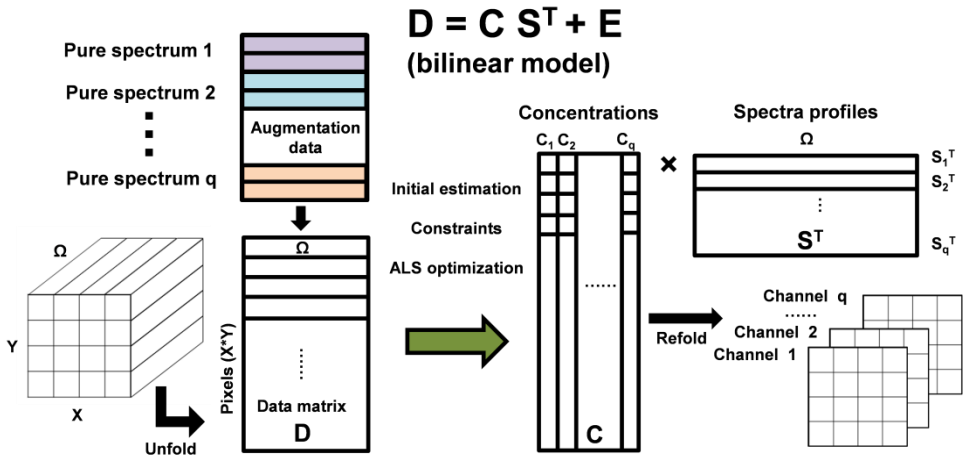


***Figure S2.*** MCR flow chart. The hyperspectral SRS image stack is unfolded into a two dimensional (2-D) data matrix D and combines with augmentation data as MCR input. Giving initial estimation of spectra, ALS algorithm decomposes data matrix D into concentration matrix C and corresponding spectra profiles $S^T$ for q components. Here, q is the number of components. The matrix C is then refolded to concentration maps for each component.

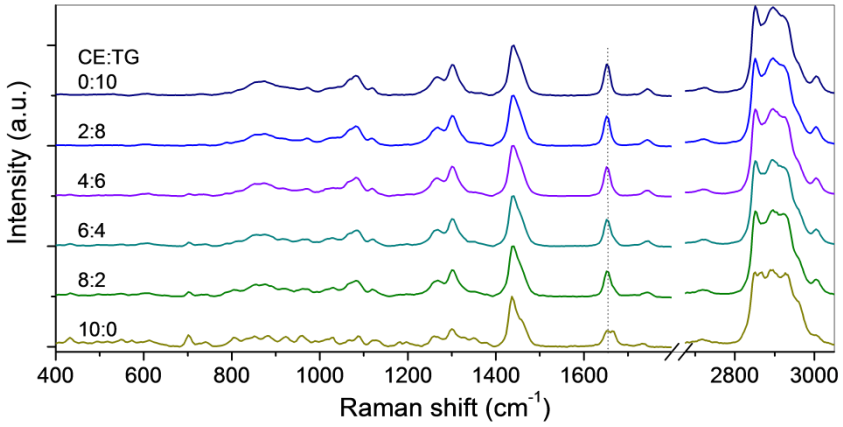


***Figure S3.*** Spontaneous Raman spectra of glyceryl trioleate and cholesteryl oleate emulsions. Dotted line indicates the Raman shift position of acyl C=C bond.

## *Supplementary Videos:*

***Movie S1.*** Hyperspectral SRS image stack of cholesterol, triglyceride and BSA mixture. The field of view of the movie is 240 μm × 240 μm.

***Movie S2.*** Hyperspectral SRS image stack of atherosclerotic artery tissue harvested from Ossabaw pigs. The field of view of the movie is 140 μm × 140 μm.

***Movie S3.*** Hyperspectral SRS image stack of atherosclerotic artery tissue where abundant LDs was found. The field of view of the movie is 100 μm × 100 μm.

## References:

[1] a) A. M. Weiner, *Rev. Sci. Instrum.* **2000**, *71*, 1929-1960; b) D. Zhang, P. Wang, M. N. Slipchenko, D. Ben-Amotz, A. M. Weiner, J. X. Cheng, *Anal. Chem.* **2013**, *85*, 98-106; c) V. V. Lozovoy, I. Pastirk, M. Dantus, *Opt. Lett.* **2004**, *29*, 775-777.

[2] M. N. Slipchenko, R. A. Oglesbee, D. Zhang, W. Wu, J.-X. Cheng, *J. Biophoton.* **2012**, *5*, 801-807.

[3] D. Zhang, M. N. Sipchenko, J. X. Cheng, *J. Phys. Chem. Lett.* **2011**, *2*, 1248-1253.

[4] a) L. Lee, M. Alloosh, R. Saxena, W. Van Alstine, B. A. Watkins, J. E. Klaunig, M. Sturek, N. Chalasani, *Hepatology* **2009**, *50*, 56-67; b) H. W. Wang, N. Chai, P. Wang, S. Hu, W. Dou, D. Umulis, L. V. Wang, M. Sturek, R. Lucht, J. X. Cheng, *Phys. Rev. Lett.* **2011**, *106*, 238106.

[5] a) J. Jaumot, R. Gargallo, A. de Juan, R. Tauler, *Chemometr. Intell. Lab.* **2005**, *76*, 101-110; b) A. de Juan, R. Tauler, *Crit. Rev. Anal. Chem.* **2006**, *36*, 163-176; c) P. N. Perera, K. R. Fega, C. Lawrence, E. J. Sundstrom, J. Tomlinson-Phillips, D. Ben-Amotz, *Proc. Natl. Acad. Sci. U.S.A.* **2009**, *106*, 12230-12234; d) J. Jaumot, R. Tauler, *Chemometr. Intell. Lab.* **2010**, *103*, 96-107; e) S. Piqueras, L. Duponchel, R. Tauler, A. de Juan, *Anal. Chim. Acta* **2011**, *705*, 182-192.